Biological Forum – An International Journal **14(1): 333-343(2022)**

ISSN No. (Print): 0975-1130
ISSN No. (Online): 2249-3239

Biosynthesis of Zinc Oxide Nanoparticle using the cyanobacterium *Chlorogloeopsis fritschii* BK (MN968818) Isolated from the Mangrove Environment of Kendrapara, Odisha and Evaluation of its Antibacterial Property

Radhakanta Nag[1], Himansu Sekhar Sahoo[2] and Saubhagya Manjari Samantaray[3]*
[1]Ph.D. Scholar, Department of Microbiology, College of Basic Science and Humanities, Odisha University of Agriculture and Technology, Bhubaneswar, (Odisha), India.
[2]Assistant Professor, Department of Chemistry, College of Basic Science and Humanities, Odisha University of Agriculture and Technology, Bhubaneswar, (Odisha), India.
[3]Assistant Professor, Department of Microbiology, College of Basic Science and Humanities, Odisha University of Agriculture and Technology, Bhubaneswar, (Odisha), India.

(Corresponding author: Saubhagya Manjari Samantaray)*
(Received 15 October 2021, Accepted 15 December, 2021)
(Published by Research Trend, Website: www.researchtrend.net)

ABSTRACT: **Multidrug resistance of bacteria towards antibiotics is a critical issue that must be addressed urgently and efficiently. In this context, nanoparticles can be opted as a suitable alternative for treating bacterial diseases. Recently, biosynthesized metal nanoparticles have been recommended as viable alternatives as their methods of preparations are precise and environmental-friendly for a cost-effective scale-up. For the biosynthesis of nanoparticles, a greater diversity of microbiota has been used, among which cyanobacteria are considered a valuable source due to their bioactive compound contents. In this regard, a cyanobacterium is identified as *Chlorogloeopsis fritschii* BK (MN968818) by 16S rRNA sequencing, isolated from the Mahanadi mangrove environment of Kendrapara, Odisha. It has been used for ZnO NPs synthesis in vitro. Moreover, the biosynthesized ZnO NPs are characterized by UV-Vis spectroscopy, X-ray diffraction (XRD), zeta potential measurement, FTIR, SEM-EDS. The antibacterial potency of the biosynthesized NPs has been studied on *E. coli* (MCC3671) and *B. cereus* (MCC1086). The UV-Vis spectrum shows an absorption peak at 368 nm for surface plasmon resonance. The hydrodynamic diameter was 45.03nm, and the zeta potential was -10mV for the synthesized NPs. FTIR provides evidence that the bio-functional groups of metabolites in *Chlorogloeopsis fritschii* BK (MN968818) act as viable reducing, capping, and stabilizing agents for the ZnO NPs. The crystalline-shaped ZnO NPs were observed from the SEM images, and EDS analysis confirms zinc as the primary constituent elements of the NPs. Antibacterial activity of 5 mg/ml, 10 mg/ml, and 20 mg/ml of ZnO NPs aliquots have been studied against *Escherichia coli* (MCC 3671) and *Bacillus cereus* (MCC 1086) in comparison to the commercial antibiotic ampicillin with sulbactam, respectively. The maximum MIC value has been found to be 10 mg/mL for both the strain and clear zone of 20 mm and 18 mm are observed in *Bacillus cereus* (MCC 1086) and *E. coli* (MCC 3671), respectively.**

Keywords: Biosynthesis, mangrove environment, cyanobacterium, indigenous, ZnO NP, antibacterial assay.

INTRODUCTION

Nanoscale technology has emerged as a new field of study, synthesizing nanoparticles for various applications, including catalysis, electrochemistry, biomedicine, pharmaceutics, and food technology (Salih *et al*., 2021). Physical and chemical processes such as photochemical, radiation, and chemical precipitation approaches are being utilized to synthesize nanoparticles. However, the employment of these procedures is not eco-friendly, expensive, and hazardous (Abdelgawad, 2017; Ahmed *et al*., 2017). In contrast, NPs can be produced using a biosynthetic method utilizing plant extracts and microbial communities (bacteria, fungi, algae, etc.). This method is less hazardous than physical and chemical methods (Bandeira *et al*., 2020). It is biocompatible, cost-effective, and safe (Pugazhendhi *et al*., 2019). Environmental safety is a key to sustainable climate, is the foremost priority, and has a more significant role in disease control and healthcare-associated infections (Ahmed *et al*., 2016). The development of NPs for their application in consumer healthcare, space, food, and the cosmetic industry has been aided by adopting green and environmentally friendly synthesis methods. Moreover, nanoparticles play a significant role in reducing the overuse of antibiotics employed mainly to treat pathogenic strains. Inorganic metal oxide nanoparticles such as TiO_2, CuO, and ZnO have been synthesized and employed in many investigations to treat infectious and deadly diseases. ZnO NPs are of great interest among metal oxide nanoparticles as their

production & preparation are safe and least expensive. Moreover, it is an n-type semiconducting metal oxide that has received a lot of interest in recent years because of its wide variety of applications in biomedical systems. ZnO was enlisted as GRAS (generally recognized as safe) metal oxide by US FDA (Ebadi *et al*., 2019; Patrinoiu *et al*., 2016; Shah *et al*., 2015). A bio-based ZnO NP is an eco-friendly alternative to conventional drugs. As natural products have become more prevalent, their potential has been acknowledged in agrochemicals, pharmaceuticals. They can be an alternative source of bioactive compounds to reduce metal ions and control several diseases in crops and humans (Borges *et al*., 2018; Mulabagal & Tsay, 2004). In this context, plants, algae, and microbes are attractive candidates for nanoparticle manufacturing because they contain several bioactive molecules (Khalid *et al*., 2019). Among all other microorganisms, Cyanobacteria are of particular interest in the synthesis of NPs because they are a potential source of new compounds with significant biotechnological value (Ebadi *et al*., 2019; Rastogi & Sinha, 2009). Cyanobacterial culture & biomass production system requires substantially less cultivation time than the crop plants and has high biomass capacity than other microbes (Correa *et al*., 2017). They can be used to make silver, platinum, gold, and palladium nanoparticles with biotechnological applications (Brayner *et al*., 2007). Cyanobacteria are used to produce nanoparticles (Pt, Pd, Ag, and Au) either intracellularly or extracellularly (Hamouda *et al*., 2019). Cyanobacterial extracts like polysaccharides and phycocyanin were used to produce AgNPs (Patel *et al*., 2015). Ebadi *et al*. (2019) have utilized *Nostoc* sp. EA03 to synthesize ZnO NPs. (El-Belely *et al*., 2021) have synthesized green ZnO NPs using *Arthrospira platensis*. Moreover, cyanobacteria are available in almost all habitats. But mangrove ecosystem has a rich diversity of novel cyanobacterial communities because of its unique environment. The mangrove environment is situated where terrestrial and marine ecosystems are merged. This interface mainly plays a critical role in creating and maintaining a unique ecosystem. Diverse forms of cyanobacteria are reported from the mangrove environment possessing a great variety of biotechnologically viable products. In coastal regions, the changes in microalgal species composition frequently occur under various physical, chemical, biological (overall interactions of organisms) present in that niche (Akase *et al*., 1999). Various biomolecules, such as enzymes and proteins, are involved in the biogenic synthesis of ZnO NPs by cyanobacteria. The metabolites secreted are associated with the determination of form, size, dispersity, and stability of ZnO NPs. The Mahanadi Delta mangrove region in Odisha (longitude 87^{o} 30' E and 87^{o} 06' E, and latitude 20^{o} 30' N and 20^{o} 50' N) is situated from Hansua in the North to the Jamboo river in the East. Several cyanobacterial strains such as *Cylindrospermom* sp., *Calothrix* sp., *Hapalosiphon* sp., *Phormidium* sp., *Microcystis* sp., *Anabaena* sp., *Oscilatoria* sp., and *Nostoc* sp., have already been reported in the area (Dash *et al*., 2020). Hence, the present work includes the isolation of a potential indigenous cyanobacterium from this mangrove environment, synthesis of ZnO NPs using this cyanobacterium, and antibacterial assay of the organism against two major clinical bacterial pathogens, *B. cereus* (MCC 1086) and *E. coli* (MCC3671).

MATERIAL AND METHODS

Isolation, optimization, and maintenance of the pure culture. Algal samples were collected from the Mahanadi delta mangrove area (Fig. 1b) of Kendrapara district, Odisha. Water temperature and pH were recorded during sample collection using a portable thermometer and pH meter. Samples were collected from the rhizospheric soil, bark, and epiphytic form attached to the pneumatophores of mangrove vegetation. All the collected samples were washed adequately with running tap water and kept in different flasks containing various nutrient media such as Allen and Arnon, BG11, Bold's Basal, and Chu's no.10 medium. After 6 days, visible clear green cells appeared on the surface of the container, which was then safely plated on respective agar plates containing various nutrient media for their isolation and purification. Subsequently, different cultures were allowed to grow for 6 to 8 days. Repeated culture and subculture practices were followed to obtain pure culture of the algal strain. Later, the pure cultures (BK, BK2, and BK3) from the petri-plates were transferred to 250 mL flasks containing 100mL of Bold's Basal medium and maintained under laboratory conditions temperature 27± 2°C and 24000lux light intensity.

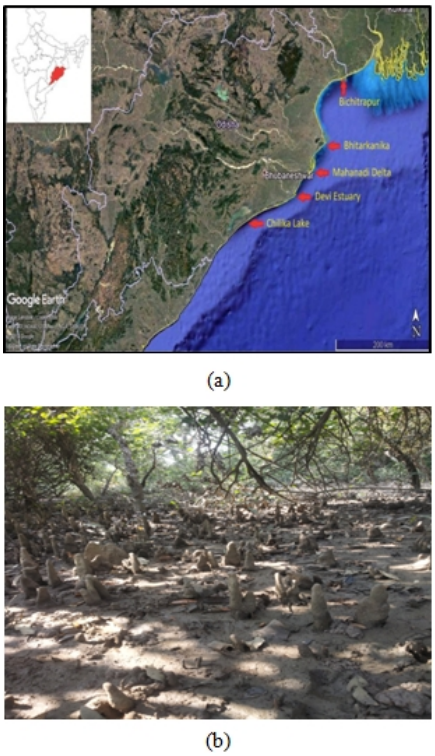

(a)

(b)

Fig. 1. Map of the sampling site (a) and (b) Mahanadi delta Mangrove region.

The mass cultures were done using cool fluorescent lights by providing 12 h of light and 12 h of dark conditions under laboratory conditions. BK has been selected for further study among the three isolated strains because of its maximum biomass production (dry weight) during its growth under laboratory conditions.

Morphological identification. For morphological characterization of cyanobacteria, it was observed under the microscope (LABOVISION, T/F, SENSE i 4000) and scanning electron microscopy (Hitachi S3400N) at CIF, OUAT, Bhubaneswar.

Molecular identification of the selected cyanobacterium. 16S rRNA sequencing was conducted for the identification of the selected isolate. DNA isolation was performed using the Qiagen DNeasy Plant Mini Kit (catalog no. 69104). DNA quality was checked and quantified using a gel documentation system and the nano-drop method, respectively. The maximum likelihood method was used for molecular phylogenetic analysis, based on the Tamura-Nei model (Tamura & Nei, 1993). The evolutionary history of the taxa was estimated by a bootstrap consensus tree assessed from 100 replicates (Kumar *et al.*, 2016). Next to the branches is the percentage of duplicate trees in which the related taxa clustered together in the bootstrap test (100 repetitions) (Felsenstein, 1992). Evolutionary studies were conducted using MEGA7 software (Kumar *et al.*, 2018).

Preparation of cell-free extract. The biomass was collected and lyophilized (MAC, LGJ33 (RB), F.D.6) for 12 hours. The cell-free extract was obtained by dissolving 10g of dried biomass in deionized water (100ml) with a slight modification of Ebadi et al. (2019); El-Naggar *et al.* (2018) by adding 100 ml distilled water heated up to 100 °C for 20 minutes, and then it was filtered using Whatman 41 filter paper (Ebadi, Zolfaghari *et al.*, 2019; El-Naggar *et al.*, 2018). The *Chlorogloeopsis fritschii* BK (MN968818) extract was preserved at 4°C for subsequent evaluation.

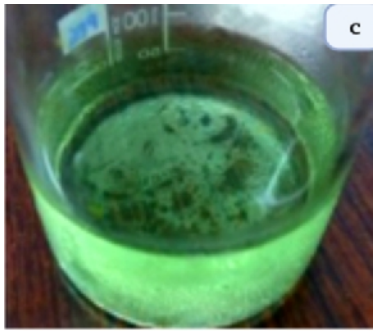

Fig. 1. (c) Cell-free extract.

Synthesis of ZnO NPs in a green manner utilizing the cell-free extract. A 75ml zinc acetate dihydrate [Zn $(CH_3COO)_2 \cdot 2H_2O$)] precursor (3mM) At 58°C, the solution was combined with 25 mL of cyanobacterial extract and stirred for an hour at 60°C at 150rpm. It was then collected and washed several times using ultrapure water and dried at 60°C for 24 hours and green synthesized ZnO NPs were obtained by heating at 100°C for 8 hours (Azizi *et al.*, 2014; Sanaeimehr *et al.*, 2018; Khalafi *et al.*, 2019).

Characterization

UV–vis absorbance of ZnO NPs. UV-vis spectrophotometer (Model 3080F) was used to monitor ZnO NPs concentrations at central laboratory, OUAT, Bhubaneswar, Odisha. The absorption spectrum was obtained at a wavelength range of 200 to 800 nm. The use of UV–visible spectra to analyse various NPs has proven to be quite efficient (Al-Kordy *et al*., 2021).

Dynamic light scattering (DLS) analysis for ZnO NPs. A "particle size analyzer" (Anton paar, Litesizer 500) was used to measure the surface charge and the size distribution of ZnO NPs at CIF, OUAT, Bhubaneswar, India. Zeta potential is the net surface charge of ZnO NPs (Al-Kordy *et al*., 2021).

FTIR analysis. The functional groups responsible for reducing zinc ions and stabilizing ZnO NPs were detected using FTIR (FTIR, Perkin Elmer Inc., USA) in the range of 400–4000 cm^{-1} at CIF OUAT, Bhubaneswar, India. The spectrum was recorded according to Iravani *et al.* (Iravani & Varma, 2020).

Scanning electron microscopy. Scanning electron microscopy SEM (SEM-EDS) (Hitachi S3400N) was used to evaluate the morphology and the elemental analysis. At CIF, OUAT, Bhubaneswar, India, biosynthesized ZnO NPs were employed for SEM analysis.

X-ray diffraction (XRD) analysis. The X-ray diffraction (XRD) was carried out to determine the hexagonal crystal structure of cyanobacterial-based ZnO-NPs synthesized using the cyanobacterium *Chlorogloeopsis fritschii* BK (MN968818) extract involved in the biosynthesis ZnO-NPs as per the ICSD reference 01-075-0576 pattern.

Antimicrobial assay. Following the disc diffusion approach (Kalaimurugan *et al*., 2019), the antibacterial activity of biosynthesized ZnO NPs was tested against human clinical pathogens such as *B.cereus* (MCC 1086) and *E. coli* (MCC3671) in comparison to commercial antibiotic ampicillin with sulbactam. The bacterial strains were maintained in the brain heart infusion (BHI, M210-100G HiMedia) broth, plated on Mueller Hinton Agar (MHA, MV173-500G) Hi-Media, plates. The lawn culture of bacterial strains were inoculated with different concentration of ZnO NPs (5 mg/ml ,10 mg/ml, 20 mg/ml). The plates (MHA) were then incubated for 18 hours at 37°C. The zone of inhibition (ZOI) was measured using PW114 HiAntibiotic ZoneScale ^{TM} (HiMedia) dimensions of 200 × 95mm at the end of the incubation period.

RESULT AND DISCUSSION

In recent years, the exploitation of microorganisms in the synthesis of NPs has received considerable attention as an alternative to chemical and physical methods of NPs synthesis. The utilization of biological substances from the microorganism makes way to eliminate expensive and harsh chemicals (Yusof *et al*., 2020). The Mahanadi river flowing into the north-eastern

Indian Ocean have a significant influence on the biogeochemical cycling in the nearshore waters of India. The estuaries and coastal waters have complex environmental conditions; mixing saline water with local circulation (river water) is crucial in managing the estuary nutrients (Roy *et al*., 2021). The fluvial sources play a vital role in the Bay of Bengal's nutrient distribution. The clayey and nutrient-rich mangrove soil of the Mahanadi delta provides a unique environment for various microorganisms. Cyanobacteria such as *Oscillatoria* sp., *Lyngbya* sp., *Cylindrospermom* sp., *Calothrix* sp., *Hapalosiphon* sp., *Phormidium* sp., *Microcystis* sp., *Anabaena* sp., *Oscilatoria* sp., and *Nostoc* sp., have previously been reported from this region (Dash *et al*., 2020).

Isolation, optimization, and maintenance of the pure culture. Three different cyanobacterial isolates (BK, BK1, and BK2) were isolated and maintained under laboratory condition to the laboratory condition. After growth optimization on a dry weight basis, the BK isolate is selected for further characterization due to its higher biomass production (on a dry weight basis), as shown in Fig. 2, including the flask culture and micrographs.

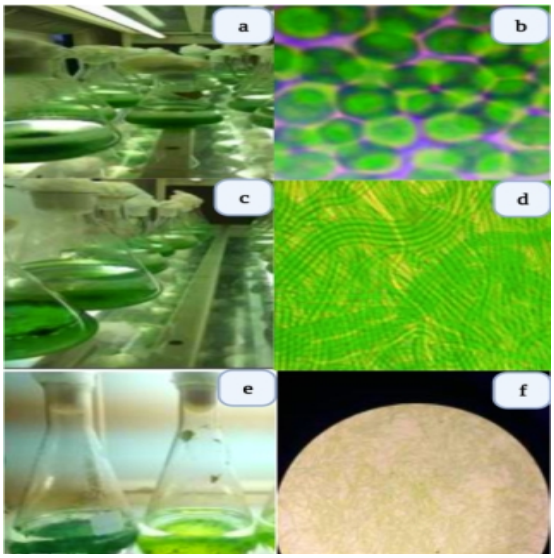

Fig. 2. (a) Flask culture of BK (b) Micrograph of BK (c) Flask culture of BK1 (d), Micrograph of BK1 (e) Flask culture of BK2 and (f) Micrograph of BK2

Molecular identification. The selected strain (BK) has been identified as *Chlorogloeopsis fritschii* BK from the 16S rRNA sequencing. It is based on the NCBI BLAST showing a percentage identity of 98.89 % and query coverage of 100% with the 16S rRNA region. The Contig sequence (FASTA) was

>BKGCGTGAGAATCTGGCTCTAGGTTCGGGAC
AACCACTGGAAACGGTGGCTAATACCGGATGT
GCCGTTATGGTGAAAGGCTAGCTGCCTAGAGA
TGAGCTCGCGTCTGATTAGCTAGATGGTGGGGT
AAGAGCCTACCATGGCGACGATCAGTAGCTGG
TCTGAGAGGATGATCAGCCACACTGGGACTGA
GACACGGCCCAGACTCCTACGGGAGGCAGCAG
TGGGGAATTTTCCGCAATGGGCGAAAGCCTGA
CGGAGCAATACCGCGTGAGGGAGGAAGGCTCT
TGGGTTGTAAACCTCTTTTCTCAGGGAAGAAGA
ATGACGGTACCTGAGGAATCAGCATCGGCTAA
CTCCGTGCCAGCGCCGCGGTAATACGGAGGAT
GCAAGCGTTATCCGGAATGATTGGGCGTAAAG
CGTCCGTAGGTGGTGATGCAAGTCTATTGTCAA
AGCGTGCGGCTCAACCGCATAAAGGCAGTGGA
AACTGTGTAACTAGAGTGCATTCGGGGCAGGG
GGAATTCCTGGTGTAGCGGTGAAATGCGTAGA
GATCAGGAAGAACACCGGTGGCGAAAGCGCCC
TGCTAGGCTGCAACTGACACTGAGGGACGAAA
GCTAGGGGAGCGAATGGGA.

From NCBI BLAST and phylogenetic tree analysis, the organism was confirmed as *Chlorogloeopsis fritschii* BK with gene bank accession number MN968818 (Fig. 4).

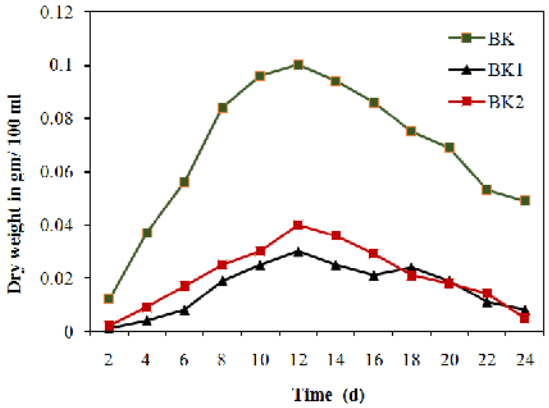

Fig. 3. Growth curve of cyanobacterial isolates BK, BK1, and BK2 on a dry cell weight basis.

Light microscopy and SEM revealed the purity and morphology of the cyanobacterial strain. Molecular analysis of 16S rRNA gene sequences of the strains disclosed that the selected cyanobacterial isolate belongs to the genus of *Chlorogloepsis fritschii* (MN968818). Similar, 16S rRNA gene sequences were followed by Ebadi *et al*., (2019) for molecular identification of cyanobacterium *Nostoc* sp. EA03 (Ebadi *et al*., 2019).

UV-Visible spectroscopy. Fig. 5 showed the UV absorption peaks of ZnO NPs. The recorded UV-Vis spectra showed a peak at 368nm, which indicated the ZnO NPs formation.

The reduction of Zn^{2+} to ZnO NPs has been confirmed by the peak at 368nm under UV–Vis spectroscopy study. The formation of such peak occurred due to the surface plasmon resonance (SPR) of biosynthesized ZnO NPs. A similar result has also been reported by Ebadi *et al*. (2021), who has used cyanobacterial (*Desertifilum* sp.) extract to synthesize ZnO NPs. Our finding is also in agreement with the results obtained by Cheng *et al*. (2020) investigation on the toxicity and genotoxicity of ZnO NPs on human lung fibroblasts and *Drosophila melanogaster*. In general, ZnO NPs show an absorption peak between 300 and 380 nm due to oxygen transfer (excitonic) (Pai *et al*., 2019) in its UV-Vis spectrum. The appearance of the broad SPR peak reveals the polydispersity of biosynthesized ZnO NPs. Likewise, prior studies of biosynthesis of ZnO NPs by

microorganisms report the absorption peak in the same range (Saravanan *et al.*, 2018; Ezealisiji *et al*., 2019).

DLS Analysis of the ZnO NPs. The dynamic light scattering analysis (DLS) indicated that the hydrodynamic size was 45.03 nm (Fig. 6 a and b). The zeta potential distribution graph indicated a negative zeta potential value of -10 mV for the biosynthesized zinc oxide NPs.

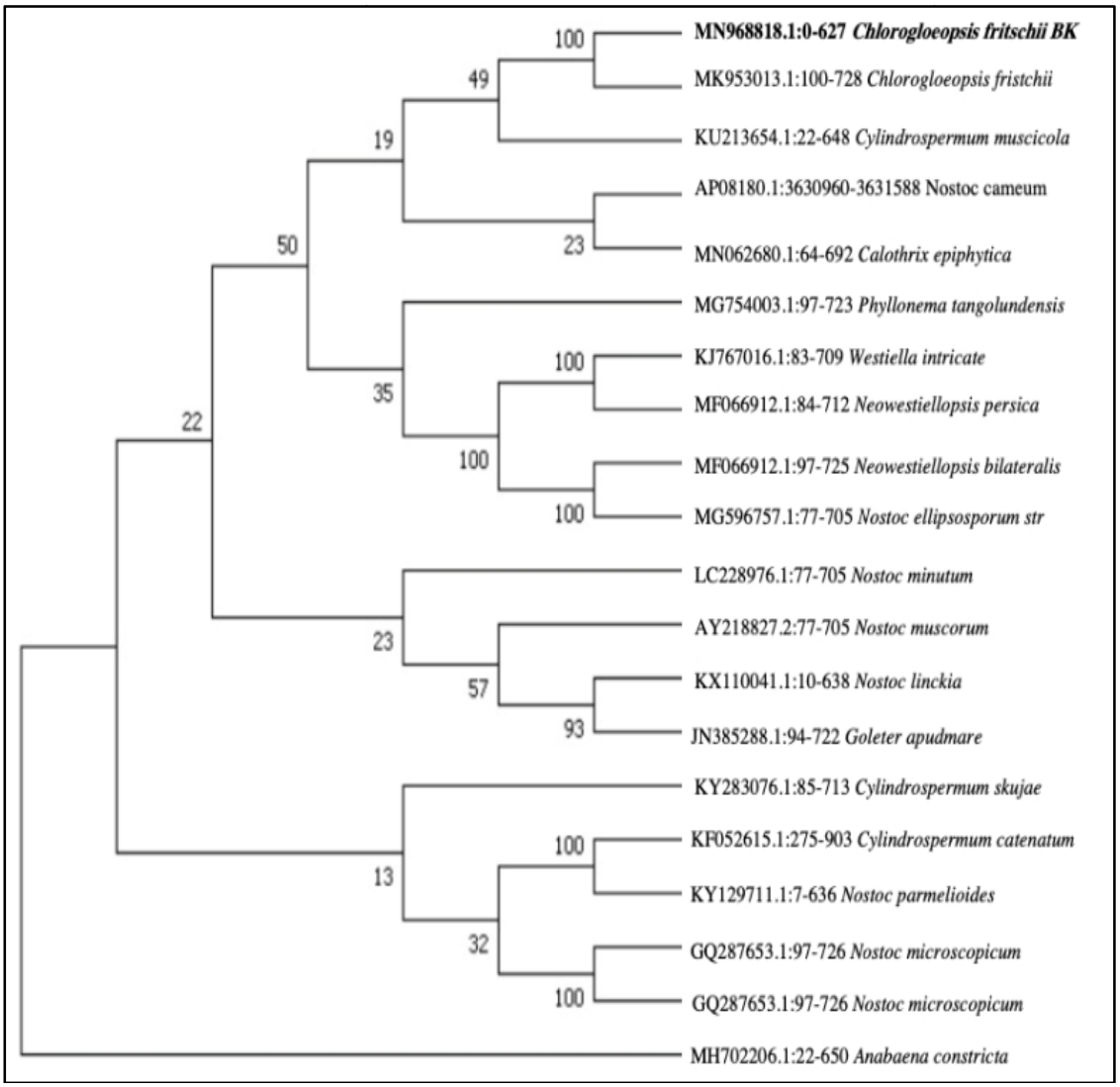

(a)

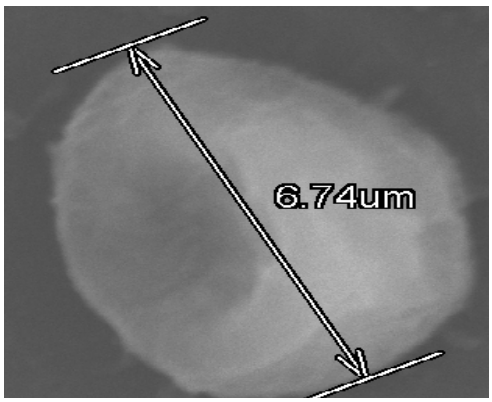

(b)

Fig. 4. (a) Phylogenetic tree of the selected BK strain and (b) SEM micrograph of the *Chlorogloepsis fritschii* BK (MN968818).

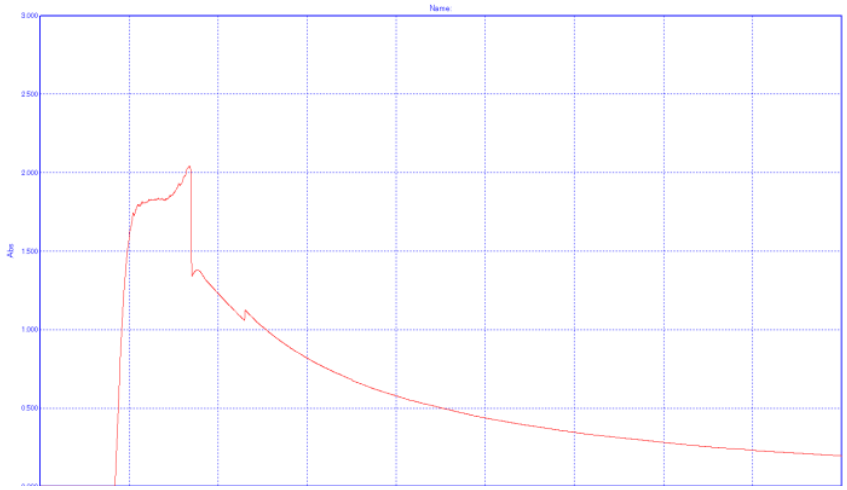

Fig. 5. UV spectroscopy analysis of ZnO NPs synthesized from cell-free extracts

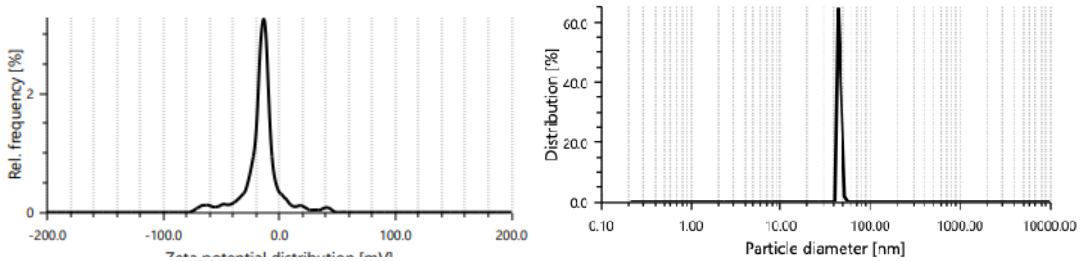

(a) (b)

Fig. 6. DLS analysis of biosynthesized ZnO NPs (a) zeta potential (-10mV) and (b) hydrodynamic diameter (45.03nm).

The hydrodynamic diameter (45.03 nm) and mono dispersed condition of biosynthesized ZnO NPs was studied using the DLS technique (Fig. 6). A similar observation has also been reported by Yusuf *et al.* (2020) on ZnO NPs while they have studied their antibacterial and biocompatibility properties. The hydrodynamic size of the biosynthesized ZnO NPs consists of a large diameter due to the measurements taken from the metal core to the attached biological compound to the particle surface. It also reveals the presence of highly mono-dispersed NPs in the suspension. ZnO NPs biosynthesized using *Chlorogloeopsis fritschii* BK (MN968818) extract has shown high negative zeta potential (-10 mV), which confirms the stability of ZnO NPs (Fig. 6). Prior to our findings, a similar observation has also been reported by Asif *et al.* (2021), where the ZnO NPs are prepared from cyanobacterium strain *Oscillatoria* sp. NCCU-369, and they have studied its antibacterial activity.

Fourier transformed infrared (FTIR) spectroscopy analysis. The Fourier Transform Infrared spectrometer (FTIR) analysis of *Chlorogloeopsis fritschii* BK (MN968818) based ZnO NPs showed different peaks at 3062.35, 2324.41, 1547.02, 1436.10, 1057.06, 688.70, 620.62, and 480.77cm^{-1}. The broad peak at 3062.35cm^{-1} indicated stretching of –O–H group (Fig. 7).

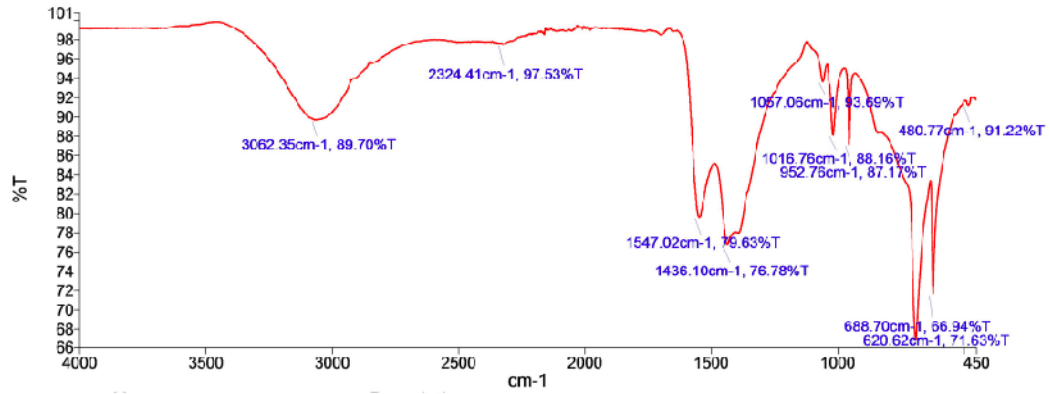

Fig. 7. FTIR analysis of ZnO NPs using *Chlorogloeopsis fritschii* BK (MN968818) extract.

The peak at 2324 cm^{-1} illustrated –C-H stretching. The band at 1547.02 cm^{-1} represented N-O stretching and the presence of nitro compounds. The band at 1436.10, 1057.06 cm^{-1} referred to the C-H bending frequency for alkane groups. The successful formation of ZnO NPs confirmed by the bands at 688.70, 620.62, and 480.77cm^{-1} for M-O stretching. FT-IR spectrum of synthesized ZnO NPs shows peaks at 687.99, 620.42, 480.77cm^{-1}, which indicated the presence of various Zn-O bending frequencies. Meanwhile, other investigations have revealed that ZnO has a variety of FTIR spectral bands at various positions 416.14 cm^{-1} (Ebadi, Zolfaghari, *et al*., 2019), 503.00 cm^{-1} (Khalafi *et al*., 2019) and 618.00 cm^{-1} (Umar *et al*., 2019). Similarly, the FT-IR analysis of the green synthesized ZnO-NPs show the Zn–O absorption peak at wavelength 782 cm^{-1} (Singh *et al*., 2019), 450 600 cm^{-1} (Fakhari *et al*., 2019), 485 cm^{-1} (Buazar *et al*., 2016), 442 cm^{-1} (Nagarajan & Arumugam Kuppusamy, 2013), 400-500 cm^{-1} (Zhang *et al*., 2011).

The peak at 3062.35 cm^{-1} attributed towards –O–H stretching frequency, and peak at 2324 cm^{-1} is for –C-H stretching frequency. The peak at 1547.02 cm^{-1} is for N-O stretching vibration of the nitro group, whereas peaks at 1436.10, 1057.06 cm^{-1} refer to the C-H bending vibration for alkane groups present in the biomolecules. These functional groups confirm biomolecules' role in reducing and stabilizing synthesized ZnO NPs (Mohd Yusof *et al*., 2019).

Scanning electron microscopy with Energy-dispersive X-ray spectroscopy. The morphology of ZnO NPs synthesized using *Chlorogloepsis fritschii* BK (MN968818) by SEM study. This gave evidence of surface characteristics of NPs and any interaction between ZnO NPs and bioactive agents. The result of SEM analysis as depicted in Fig. 8 (a). The ZnO particles were in the form of irregularly shaped crystals. Moreover, the ZnO NPs were in aggregates form due to the interaction among biomolecules capping and stabilizing the NPs. The elemental composition was also performed to assess the composition of the prepared ZnO NPs, and the response was depicted in Fig. 8 (b) ZnO NPs produced a characteristic optical observation peak between 1-10 keV approximately.

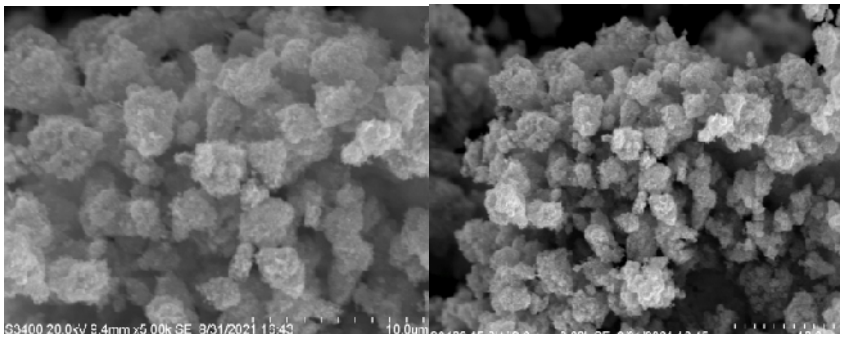

(a)

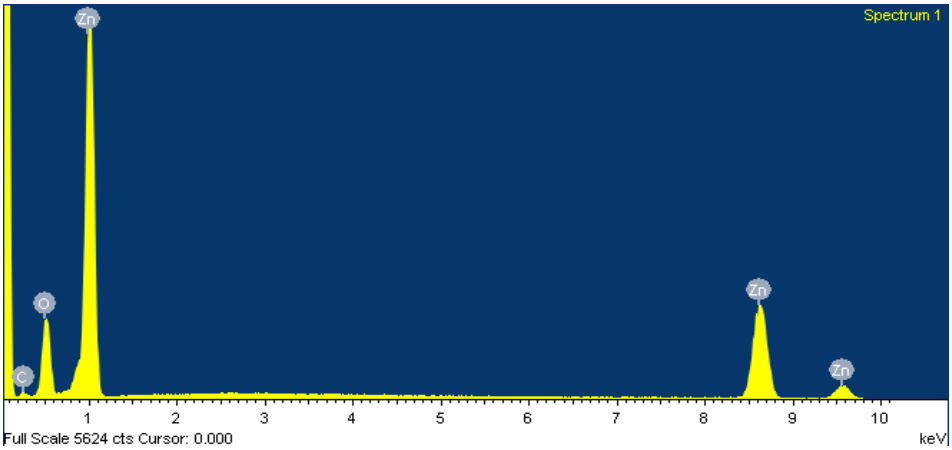

(b)

Fig. 8. (a) SEM micrograph of biosynthesized ZnO NPs using *Chlorogloepsis fritschii* BK (MN968818) extract, (b) EDX spectra of biosynthesized ZnO NPs using *Chlorogloepsis fritschii* BK (MN968818) extract.

The SEM images of the biosynthesized ZnO NPs show these are crystalline in nature and had irregular surface structures found in aggregated form (Fig. 8). The EDX spectrum confirmed the successful synthesis of the ZnO NPs as only peaks for Zn and O are observed (Fig. 9). The absence of other elements also reports the biosynthesized ZnO NPs are pure, which is also corroborated with the results from the XRD analysis. A similar finding has also been reported by other research groups (Ebadi, Reza Zolfaghari, *et al*., 2019; El-Belely

et al., 2021), while they have done their study on *Bacillus subtilis*, *Staphylococcus aureus*, *Pseudomonas aeruginosa*, *Escherichia coli*, and *Candida albicans*, respectively. They have also reported that ZnO NPs reduce as concentration is decreased, whereas the absence of impurities in the synthesized ZnO NPs is important for efficient antimicrobial activity (Mahamuni *et al*., 2019).

X-ray Diffraction (XRD) evaluation. XRD analysis was used to determine the structure of biosynthesized ZnO NPs. As per the ICSD reference 01-075-0576 pattern, significant peaks at 2θ= 31.8°, 34.5°, 36.3°, 47.6°, 56.7°, 63. 0°, 66.5°, 68.1°, 69.2°, 72.7°, 77.1°, 81.6°, 89.8° observed, were matched to (100), (002), (101), (102), (110), (013), (200), (112), (204), (004), (202), (104) and (203) planes, respectively and presented in Fig. 9. The presence of nanoparticles can be established based on the observed peaks, especially at 2θ=31.8–89.8. The high 2θ degree intensity was obtained at 36.334°.

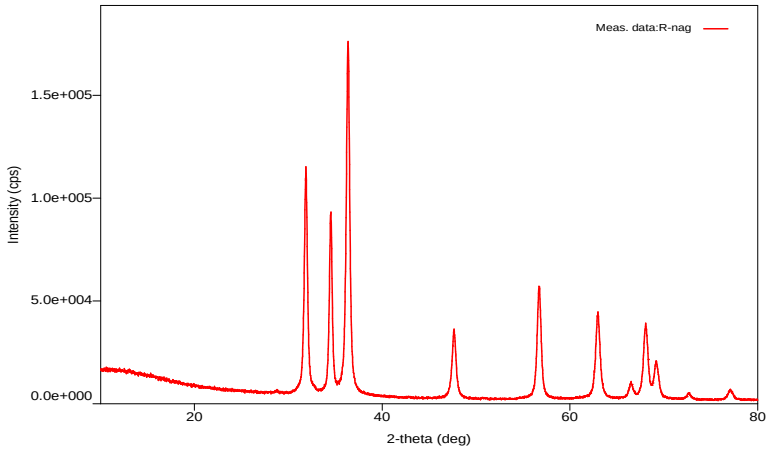

Fig. 9. XRD pattern of ZnO NPs synthesized employing *Chlorogloepsis fritschii* BK (MN968818).

The formation of crystalline nanoparticles can be established on the basis of the appearance of peaks in the range of 31.8° - 89.8° (in 2θ°) as observed from the ICSD reference pattern (Fouda *et al*., 2018; Ebadi, Reza Zolfaghari, *et al*., 2019; Sabine & Hogg, 1969). The presence of slight and extra peaks in XRD spectra may be related to the crystallization of organic substances that coated the surface of ZnO NPs (Ebadi, *et al*., 2019). The high crystalline nature of the synthesized ZnO NPs has also been observed form the high intensity of diffraction peaks (Fig. 9). No other diffraction peak has been observed in the XRD data, which suggests the synthesized ZnO NPs had high purity. This result has also been compared to the reported data for the biosynthesized ZnO NPs obtained from the extract of cyanobacterium *Nostoc* sp. EA03 and zinc acetate dihydrate (98% Zn $(CH_3COO)_2 \cdot 2H_2O$) (Ebadi, Reza Zolfaghari, *et al*., 2019).

Antibacterial activity. The antibacterial activity of the ZnO NPs was studied against *B. cereus* (MCC 1086) and *E. coli* (MCC3671) in comparison to the standard antibiotics ampicillin with sulbactam. As shown in Fig. 10, all concentrations of ZnO NPs applied had inhibitory effects on both cultures, and the zones of inhibition grew consistently as the concentration of ZnO NPs rose. The zone size for *B. cereus* (MCC 1086) ranged from 19.09mm (10mg/ml concentration) to 22.10 mm (20mg/ml concentration) (Fig. 11, 12). However, the standard antibiotic showed a zone size of 16.09mm. Hence, the MIC value for *B. cereus* (MCC 1086) was found to be 10mg/ml. Similarly, the zone size for *E. coli* (MCC3671) at 10mg/ml and 20mg/ml ZnO NPs concentration was recorded as 15.77mm and 23.92 mm, respectively. In contrast, the standard commercial antibiotic showed a zone size of 15.13 mm. 10mg/ml ZnO NPs was reported as the minimum inhibitory concentration. The bio-synthesized ZnO NPs was studied for their antibacterial activity against clinical pathogens *B. cereus* (MCC 1086) and *E. coli* (MCC3671). It has been compared with the standard antibiotic ampicillin with sulbactam, and the MIC value is found to be 10 mg/mL in both cases. Our findings are in good agreement with the reported data by Punjabi *et al*. (2018), where the antibacterial activity of ZnO NPs have been studied against *E. coli* and *B. cereus* and compared with standard antibiotic Gentamicin (Punjabi *et al*., 2018). Similar results have also been reported for the ZnO NPs from the cyanobacterial extract of *Nostoc* sp. EA03 and their antibacterial activity studies against *E. coli*, *P. aeruginosa*, and *S. aureus* (Ebadi *et al*., 2019). The biosynthesized ZnO NPs can also be used in pharmaceutical industries (El-Belely *et al*., 2021). The obtained results revealed that the biosynthesized ZnO NPs have antibacterial capabilities and cause significant damage to intracellular and extracellular bacterial components. The positive charge on the ZnO NPs neutralizes the negative charge of the bacterial cell surface, and the porin channels on the bacterial cell wall get broken, which facilitates the transfer of Zn ion into the bacterial cell (Praveena *et al*., 2020). The teichoic acid and lipid bilayer of the bacterial cells are then altered. The antigenicity of Zn ions was removed when linked to the broken porin channels of bacteria. Finally, the ZnO NPs-treated bacteria have been destroyed and stayed in the decline phase due to the depletion of critical components.

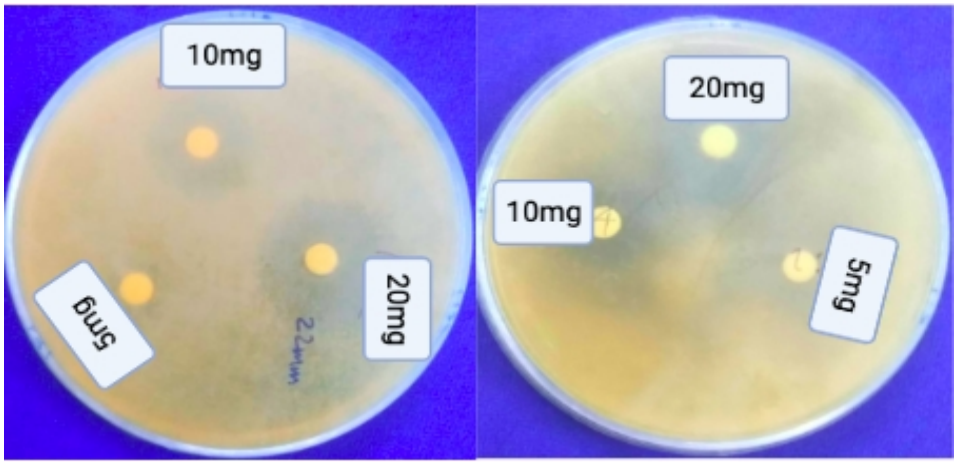

(a) (b)

Fig. 10. Antibacterial activity of ZnO NPs against (a) *B. cereus* (MCC 1086), (b) *E. coli* (MCC3671).

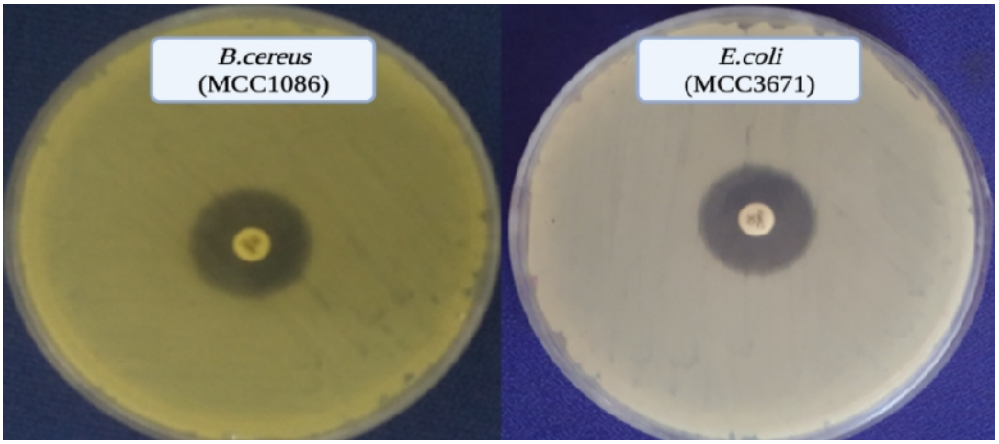

(a) (b)

Fig. 11. Antibacterial activity of antibiotic ampicillin with sulbactam against (a) *B. cereus* (MCC 1086); (B) *E. coli* (MCC3671).

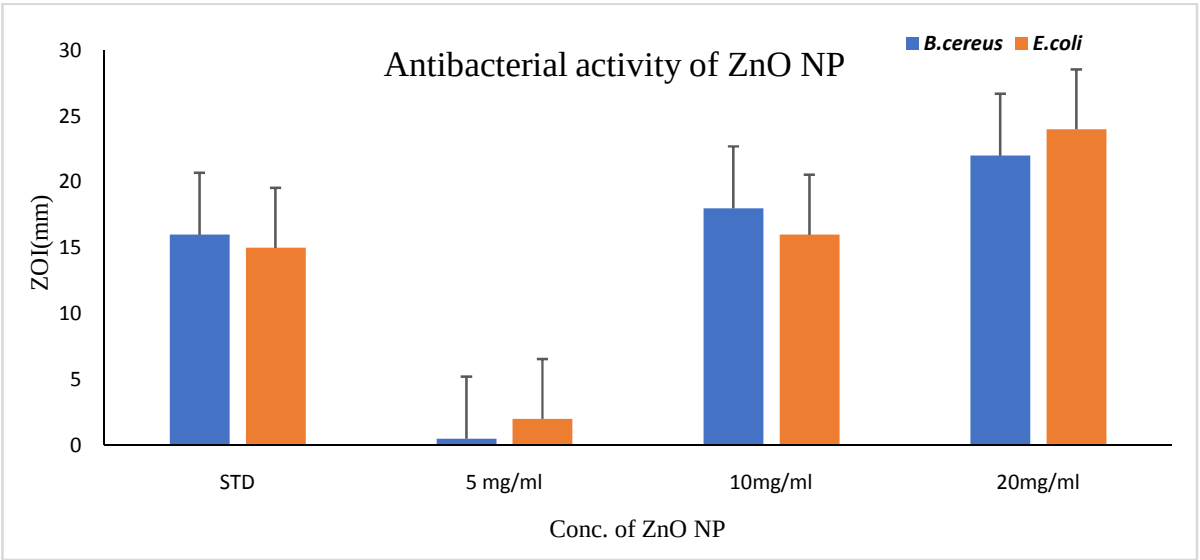

Fig. 12. Antibacterial activity of *B. cereus* (MCC 1086) and *E. coli* (MCC3671) (disc diffusion).

CONCLUSION

The utilization of cyanobacteria has paved the way for green nanotechnology, lowering the generation of unwanted and impure chemicals. The present study lays the groundwork for future research into our understanding of how the aqueous extract of *Chlorogloeopsis fristchii* BK (MN968818) collected from the Mahanadi Delta mangrove region can be used as a reducing and capping agent for the biosynthesis of ZnO NPs. The ZnO NPs characterized by UV–Vis spectroscopy, FTIR, XRD, SEM-EDS, and DLS analysis. The biosynthesized ZnO NPs demonstrated significant antibacterial activities against *B. cereus* (MCC 1086) and *E. coli* (MCC3671) in comparison to the standard antibiotic ampicillin with sulbactam. The green synthesis and high efficacy of the cyanobacterium *Chlorogloeopsis fristchii* BK (MN968818) for ZnO NPs synthesis may be helpful for its applications as an antibacterial agent to treat the infection caused by *B. cereus* (MCC 1086) and *E. coli* (MCC 3671). The benefits of using cyanobacterium extract to synthesize ZnO NPs are cost-effective, energy-efficient, environment-friendly and safe.

Acknowledgements. The present study is a portion of R. Nag's Ph.D. research. The authors would like to express their gratitude to the Central Instrumentation Facility at Odisha University of Agriculture and Technology, Bhubaneswar, Odisha, India for providing laboratory space and characterization instruments for conducting this research.
Conflict of Interest. None.

REFERENCES

Abdelgawad, A. (2017). Tamarix nilotica (Ehrenb) Bunge: A Review of Phytochemistry and Pharmacology. *Journal of Microbial & Biochemical Technology*, *09*.

Ahmed, S., Ahmad, M., Swami, B. L., & Ikram, S. (2016). A review on plants extract mediated synthesis of silver nanoparticles for antimicrobial applications: A green expertise. *Journal of Advanced Research*, *7*(1): 17–28.

Ahmed, S., Annu, Chaudhry, S. A., & Ikram, S. (2017). A review on biogenic synthesis of ZnO nanoparticles using plant extracts and microbes: A prospect towards green chemistry. *Journal of Photochemistry and Photobiology B: Biology*, *166*: 272–284.

Akase, S., Yoshikawa, T., & Sakata, T. (1999). Pigment Analysis of Marine Microalgae by TLC and HPLC Methods. *Aquaculture Science*, *47*(4): 511–518.

Al-Kordy, H. M. H., Sabry, S. A., & Mabrouk, M. E. M. (2021). Statistical optimization of experimental parameters for extracellular synthesis of zinc oxide nanoparticles by a novel haloalaliphilic *Alkalibacillus* sp.W7. *Scientific Reports*, *11*(1): 10924.

Asif, N., Fatima, S., Aziz, Md. N., Shehzadi, Zaki, A., & Fatma, T. (2021). Biofabrication and characterization of cyanobacteria derived ZnO NPs for their bioactivity comparison with commercial chemically synthesized nanoparticles. *Bioorganic Chemistry*, *113*, 104999.

Azizi, S., Ahmad, M. B., Namvar, F., & Mohamad, R. (2014). Green biosynthesis and characterization of zinc oxide nanoparticles using brown marine macroalga Sargassum muticum aqueous extract. *Materials Letters*, *116*: 275–277.

Bandeira, M., Giovanela, M., Roesch-Ely, M., Devine, D. M., & da Silva Crespo, J. (2020). Green synthesis of zinc oxide nanoparticles: A review of the synthesis methodology and mechanism of formation. *Sustainable Chemistry and Pharmacy*, *15*, 100223.

Borges, D. F., Lopes, E. A., Fialho Moraes, A. R., Soares, M. S., Visôtto, L. E., Oliveira, C. R., & Moreira Valente, V. M. (2018). Formulation of botanicals for the control of plant-pathogens: A review. *Crop Protection*, *110*: 135–140.

Brayner, R., Barberousse, H., Hemadi, M., Djedjat, C., Yéprémian, C., Coradin, T., Livage, J., Fiévet, F., & Couté, A. (2007). Cyanobacteria as Bioreactors for the Synthesis of Au, Ag, Pd, and Pt Nanoparticles via an Enzyme-Mediated Route. *Journal of Nanoscience and Nanotechnology*, *7*(8): 2696–2708.

Buazar, F., Bavi, M., Kroushawi, F., Halvani, M., Khaledi-Nasab, A., & Hossieni, S. A. (2016). Potato extract as reducing agent and stabiliser in a facile green one-step synthesis of ZnO nanoparticles. *Journal of Experimental Nanoscience*, *11*(3): 175–184.

Cheng, J., Wang, X., Qiu, L., Li, Y., Marraiki, N., Elgorban, A. M., & Xue, L. (2020). Green synthesized zinc oxide nanoparticles regulates the apoptotic expression in bone cancer cells MG-63 cells. *Journal of Photochemistry and Photobiology B: Biology*, *202*, 111644.

Correa, D. F., Beyer, H. L., Possingham, H. P., Thomas-Hall, S. R., & Schenk, P. M. (2017). Biodiversity impacts of bioenergy production: Microalgae vs. first generation biofuels. *Renewable and Sustainable Energy Reviews*, *74*: 1131–1146.

Dash, S. R., Pradhan, B., Behera, C., & Jena, M. (2020). Algal diversity of Kanjiahata lake, Nandankanan, Odisha, India. *The Journal of Indian Botanical Society*, *99*(1-2): 11–24.

Ebadi, M., Reza Zolfaghari, M., Soheil Aghaei, S., Zargar, M., Shafiei, M., Shahbani Zahiri, H., & Akbari Noghabi, K. (2019). A bio-inspired strategy for the synthesis of zinc oxide nanoparticles (ZnO NPs) using the cell extract of cyanobacterium Nostoc sp. EA03: From biological function to toxicity evaluation. *RSC Advances*, *9*(41): 23508–23525.

El-Belely, E. F., Farag, M. M. S., Said, H. A., Amin, A. S., Azab, E., Gobouri, A. A., & Fouda, A. (2021). Green Synthesis of Zinc Oxide Nanoparticles (ZnO-NPs) using Arthrospira platensis (Class: Cyanophyceae) and Evaluation of their Biomedical Activities. *Nanomaterials*, *11*(1).

El-Naggar, N. E.-A., Hussein, M. H., & El-Sawah, A. A. (2018). Phycobiliprotein-mediated synthesis of biogenic silver nanoparticles, characterization, in vitro and in vivo assessment of anticancer activities. *Scientific Reports*, *8*(1): 8925.

Ezealisiji, K. M., Siwe-Noundou, X., Maduelosi, B., Nwachukwu, N., & Krause, R. W. M. (2019). Green synthesis of zinc oxide nanoparticles using *Solanum torvum* (L) leaf extract and evaluation of the toxicological profile of the ZnO nanoparticles–hydrogel composite in Wistar albino rats. *International Nano Letters*, *9*(2): 99–107.

Fakhari, S., Jamzad, M., & Kabiri Fard, H. (2019). Green synthesis of zinc oxide nanoparticles: A comparison. *Green Chemistry Letters and Reviews*, *12*(1): 19–24.

Felsenstein, J. (1992). Phylogenies from restriction sites: A maximum-likelihood approach. *Evolution*, *46*(1): 159–173.

Fouda, A., EL-Din Hassan, S., Salem, S. S., & Shaheen, T. I. (2018). In-Vitro cytotoxicity, antibacterial, and UV protection properties of the biosynthesized Zinc oxide nanoparticles for medical textile applications. *Microbial Pathogenesis*, *125*: 252–261.

González-Medina, M., & Medina-Franco, J. L. (2019). Chemical Diversity of Cyanobacterial Compounds: A Chemoinformatics Analysis. *ACS Omega*, *4*(4): 6229–6237.

Hamouda, R. A., Hussein, M. H., Abo-elmagd, R. A., & Bawazir, S. S. (2019). Synthesis and biological characterization of silver nanoparticles derived from the cyanobacterium *Oscillatoria limnetica*. *Scientific Reports*, *9*(1): 13071.

Iravani, S., & Varma, R. S. (2020). Bacteria in Heavy Metal Remediation and Nanoparticle Biosynthesis. *ACS Sustainable Chemistry & Engineering*, *8*(14): 5395–5409.

Kalaimurugan, D., Vivekanandhan, P., Sivasankar, P., Durairaj, K., Senthilkumar, P., Shivakumar, M. S., & Venkatesan, S. (2019). Larvicidal activity of silver nanoparticles synthesized by *Pseudomonas fluorescens* YPS3 isolated from the Eastern Ghats of India. *Journal of Cluster Science*, *30*(1): 225–233.

Khalafi, T., Buazar, F., & Ghanemi, K. (2019). Phycosynthesis and Enhanced Photocatalytic Activity of Zinc Oxide Nanoparticles Toward Organosulfur Pollutants. *Scientific Reports*, *9*(1): 6866.

Khalid, H. F., Tehseen, B., Sarwar, Y., Hussain, S. Z., Khan, W. S., Raza, Z. A., Bajwa, S. Z., Kanaras, A. G., Hussain, I., & Rehman, A. (2019). Biosurfactant coated silver and iron oxide nanoparticles with enhanced anti-biofilm and anti-adhesive properties. *Journal of Hazardous Materials*, *364*: 441–448.

Kumar, S., Stecher, G., Li, M., Knyaz, C., & Tamura, K. (2018). MEGA X: Molecular Evolutionary Genetics Analysis across Computing Platforms. *Molecular Biology and Evolution*, *35*(6): 1547–1549.

Kumar, S., Stecher, G., & Tamura, K. (2016). MEGA7: Molecular Evolutionary Genetics Analysis Version 7.0 for Bigger Datasets. *Molecular Biology and Evolution*, *33*(7): 1870–1874.

Mahamuni, P. P., Patil, P. M., Dhanavade, M. J., Badiger, M. V., Shadija, P. G., Lokhande, A. C., & Bohara, R. A. (2019). Synthesis and characterization of zinc oxide nanoparticles by using polyol chemistry for their antimicrobial and antibiofilm activity. *Biochemistry and Biophysics Reports*, *17*: 71–80.

Mohd Yusof, H., Mohamad, R., Zaidan, U. H., & Abdul Rahman, N. A. (2019). Microbial synthesis of zinc oxide nanoparticles and their potential application as an antimicrobial agent and a feed supplement in animal industry: A review. *Journal of Animal Science and Biotechnology*, *10*(1): 57.

Mulabagal, V., & Tsay, H. S. (2004). Plant Cell Cultures—An Alternative and Efficient Source for the Production of Biologically Important Secondary Metabolites. *International Journal of Applied Science and Engineering*, *2*(1): 29–48.

Nagarajan, S., & Kuppusamy, K. A. (2013). Extracellular synthesis of zinc oxide nanoparticle using seaweeds of gulf of Mannar, India. *Journal of nanobiotechnology*, *11*(1): 1-11.

Pai, S., H, S., Varadavenkatesan, T., Vinayagam, R., & Selvaraj, R. (2019). Photocatalytic zinc oxide nanoparticles synthesis using *Peltophorump terocarpum* leaf extract and their characterization. *Optik*, *185*, 248–255.

Patel, V., Berthold, D., Puranik, P., & Gantar, M. (2015). Screening of cyanobacteria and microalgae for their ability to synthesize silver nanoparticles with antibacterial activity. *Biotechnology Reports*, *5*: 112–119.

Patrinoiu, G., Calderón-Moreno, J. M., Chifiriuc, C. M., Saviuc, C., Birjega, R., & Carp, O. (2016). Tunable ZnO spheres with high anti-biofilm and antibacterial activity via a simple green hydrothermal route. *Journal of Colloid and Interface Science*, *462*: 64–74.

Praveena, V., Venkatalakshmi, S., Alharbi, N. S., Kadaikunnan, S., Khaled, J. M., & Govindarajan, M. (2020). Identification of a novel antibacterial protein from hemolymph of freshwater zooplankton Mesocyclops leuckarti. *Saudi Journal of Biological Sciences*, *27*(9): 2390–2397.

Pugazhendhi, A., Prabhu, R., Muruganantham, K., Shanmuganathan, R., & Natarajan, S. (2019). Anticancer, antimicrobial and photocatalytic activities of green synthesized magnesium oxide nanoparticles (MgONPs) using aqueous extract of Sargassum wightii. *Journal of Photochemistry and Photobiology B: Biology*, *190*: 86–97.

Punjabi, K., Mehta, S., Chavan, R., Chitalia, V., Deogharkar, D., & Deshpande, S. (2018). Efficiency of Biosynthesized Silver and Zinc Nanoparticles against Multi-Drug Resistant Pathogens. *Frontiers in Microbiology*, *9*,

Rastogi, R. P., & Sinha, R. P. (2009). Biotechnological and industrial significance of cyanobacterial secondary metabolites. *Biotechnology Advances*, *27*(4): 521–539.

Roy, R., Naik, R. K., D'Costa, P. M., Nagamani, P. V., & Choudhury, S. B. (2021). Nutrient Cycling and Seasonal Dynamics of Primary Production in Nearshore Waters of East Coast of India. In *Estuarine Biogeochemical Dynamics of the East Coast of India* (pp. 165–181). Springer.

Sabine, T. M., & Hogg, S. (1969). The wurtzite Z parameter for beryllium oxide and zinc oxide. *Acta Crystallographica Section B: Structural Crystallography and Crystal Chemistry*, *25*(11): 2254–2256.

Salih, A. M., Al-Qurainy, F., Khan, S., Tarroum, M., Nadeem, M., Shaikhaldein, H. O., Gaafar, A.-R. Z., & Alfarraj, N. S. (2021). Biosynthesis of zinc oxide nanoparticles using Phoenix dactylifera and their effect on biomass and phytochemical compounds in *Juniperus procera*. *Scientific Reports*, *11*(1): 19136.

Sanaeimehr, Z., Javadi, I., & Namvar, F. (2018). Antiangiogenic and antiapoptotic effects of green-synthesized zinc oxide nanoparticles using Sargassum muticum algae extraction. *Cancer Nanotechnology*, *9*(1): 3.

Saravanan, M., Gopinath, V., Chaurasia, M. K., Syed, A., Ameen, F., & Purushothaman, N. (2018). Green synthesis of anisotropic zinc oxide nanoparticles with antibacterial and cytofriendly properties. *Microbial Pathogenesis*, *115*: 57–63.

Shah, M., Fawcett, D., Sharma, S., Tripathy, S. K., & Poinern, G. E. J. (2015). Green Synthesis of Metallic Nanoparticles via Biological Entities. *Materials*, *8*(11): 7278–7308.

Singh, J., Kaur, S., Kaur, G., Basu, S., & Rawat, M. (2019). Biogenic ZnO nanoparticles: A study of blueshift of optical band gap and photocatalytic degradation of reactive yellow 186 dye under direct sunlight. *Green Processing and Synthesis*, *8*(1): 272–280.

Tamura, K., & Nei, M. (1993). Estimation of the Number of Nucleotide Substitutions in the Control Region of Mitochondrial DNA in Humans and Chimpanzees'. *Molecular Biology and Evolution*, *10*(3): 15.

Umar, H., Kavaz, D., & Rizaner, N. (2019). Biosynthesis of zinc oxide nanoparticles using Albizia lebbeck stem bark, and evaluation of its antimicrobial, antioxidant, and cytotoxic activities on human breast cancer cell lines. *International Journal of Nanomedicine*, *14*: 87.

Zhang, G., Shen, X., & Yang, Y. (2011). Facile Synthesis of Monodisperse Porous ZnO Spheres by a Soluble Starch-Assisted Method and Their Photocatalytic Activity. *The Journal of Physical Chemistry C*, *115*(15): 7145–7152.

How to cite this article: Radhakanta Nag, Himansu Sekhar Sahoo and Saubhagya Manjari Samantaray (2022). Biosynthesis of Zinc Oxide Nanoparticle using the cyanobacterium *Chlorogloeopsis fritschii* BK (MN968818) Isolated from the Mangrove Environment of Kendrapara, Odisha and Evaluation of its Antibacterial Property. *Biological Forum – An International Journal*, *14*(1): 333-343.